Effect of Stray Current on Corrosion Behavior of Reinforcing Steel: Importance of Cell Geometry and Orientation with Respect to the Electrical Field

Zhipei Chen and Dessi A. Koleva
Faculty of Civil Engineering and Geoscience, Delft University of Technology, Material and Environment Section, Stevinweg 1, 2628 CN Delft, The Netherlands
Email: {z.chen-1, D.A.Koleva}@tudelft.nl

***Abstract*—Stray current circulating in reinforced concrete structures may initiate corrosion or accelerate existing corrosion processes on embedded reinforcement. In some cases, the range of dangerous or unwanted interactions of stray currents under favorable conditions (environment), is much broader than is generally recognized. All these show that investigation of the effects of stray current on the corrosion behavior of steel is necessary and significant. In this work, the tested level of stray current was 3 mA/cm^2, and the type of samples were reinforced mortar cubes (40 mm×40 mm×40 mm). To investigate the corrosion behavior of embedded steel undergoing stray current, the evaluation indicators adopted were OCP (Open Circuit Potential), Polarization resistance (R_p) derived through LPR (Linear Polarisation Resistance), and electrochemical parameters recorded through EIS (Electrochemical Impedance Spectroscopy) and PDP (Potentio-Dynamic Polarization). The recorded electrochemical response aimed to elucidate the importance of cell geometry i.e. the effect of steel orientation with respect to the electrical field (placed parallel or orthogonal to the current direction). It was found that the geometrical position of the steel bar is of significant importance and determines the level of stray current-induced degradation.**

***Index Terms*—stray current, corrosion, electrochemistry, reinforcing steel**

I. Introduction

The corrosion of steel bars, embedded in concrete, is one of the principal causes of deterioration of Reinforced Concrete (RC) structures, especially when they are in contact with corrosive environment. Until now, factors causing infrastructure corrosion (Cl^-, carbonation, sulfates and microbiology, etc.) have been investigated by different scholars in different aspects. However, the effects of stray current are somewhat neglected or less reported, although the range of unwanted interactions of stray currents under favourable conditions are much broader than generally recognized [1]-[4]. Stray current arising from power sources and then circulating in metal structures may initiate corrosion or even accelerate existing corrosion processes [2].

Stray current can originate from electrified traction system, offshore structure, marine platform, cathodic protection system, etc., [2], [5]-[13]. The most frequent source of stray current are electrified traction systems (electrical trains, tram systems or underground trains). In these systems, the current drawn by the vehicles returns to the traction power sub-station through the running rails. This concept, besides forming part of the signaling circuit for controlling the train movements, is used as the current return circuit path, together with return conductors [2], [8], [9], [11], [13]. However, owing to the longitudinal resistance of the rails and their imperfect insulation to the ground, part of the return current leaks out from the running rails, i.e. stray current forms. The leaking-out stray current, returns to the traction power substation through the ground and underground metallic structures (such as steel re-bars in concrete, pipelines, etc.). Such situation can be potentially very harmful for underground reinforced concrete structures for example, where despite the high concrete resistivity, the steel reinforcement provides a good conductive path.

The surface of the corroding steel functions as a mixed electrode, a "composite" of anodes and cathodes, electrically connected through the body of steel itself. On this surface the coupled anodic and cathodic reactions take place, along with concrete pore water functioning as an aqueous medium, or a complex electrolyte [14]. Reactions at the anodes and cathodes are broadly referred to as half-cell reactions: the anodic reaction is the oxidation process, which results in dissolution or loss of the metal, whilst the cathodic reaction is the reduction of dissolved oxygen, forming hydroxyl ions.

For steel embedded in concrete, the possible anodic reaction, depending on the pH of interstitial electrolyte, presence of aggressive anions, and the existence of an appropriate electrochemical potential at the steel surface is Eq. (1);

$$Fe \rightarrow Fe^{2+} + 2e^- \quad (1)$$

Manuscript received October 21, 2016; revised November 8, 2016.

doi: 10.18178/ijscer.6.2.93-100

The possible cathodic reactions depend on the availability of O_2 and on the pH in the vicinity of the steel surface. The most likely reaction is Equation (2).

$$\frac{1}{2}O_2+H_2O+2e^- \rightarrow 2OH^- \quad (2)$$

In concrete, oxygen is usually able to penetrate through the pores and micro-cracks into the proximity of steel surface and the over-potential for oxygen reduction reaction is low, making this reaction the prevailing cathodic reaction [15]-[17].

Different types of reinforced concrete structures may be subjected to stray current leaking from the rails, such as viaducts, bridges and tunnels of the railway networks or structures placed in the neighborhoods of railways [18]-[21]. Here, the concrete is the electrolyte and the reinforcing bars or pre-stressing wires embedded in concrete can pick up the stray current. A comparison with stray current induced corrosion of pipelines, the issue of stray current-induced corrosion in reinforced concrete has relatively more problems to deal with, considering the interaction between steel surface and surrounding concrete matrix, i.e. the steel-concrete interface. Additionally, stray current can also affect the microstructural properties of the concrete matrix [22].

The concept of stray current in relation to reinforcement corrosion in concrete structures is illustrated in Fig. 1, where stray current (Is) originates from a DC electrical source, finds an alternative path through the soil and concrete, then is picked up by the reinforcement if appropriate conditions are present.

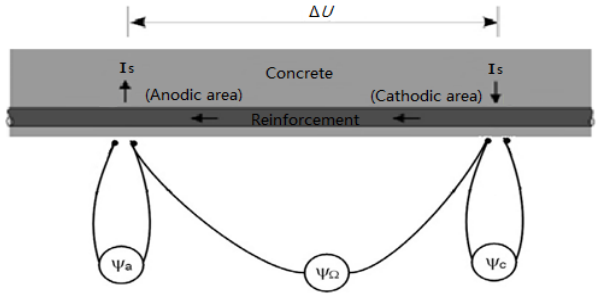

Figure 1. Schematic representation of the electrical interference on reinforcement in concrete.

Interference from stray current, flowing through surrounding soil and concrete matrix, may impose a significant effect on the electrochemical reactions (Eqs. 1 and 2), occurring on the surface of the reinforcement in underground concrete structures. Depending on the direction (sign) of the current, the electrochemical reactions stimulated by stray currents and their effects are as follows: At the point where the stray current enters the reinforcement (cathodic area), anodic reaction is depressed and the cathodic reaction is in domination (generally oxygen reduction for this environment) due to cathodic polarization. In general this will be beneficial (protecting steel), except for extreme cases where Alkali-Silica-Reaction (ASR) and loss of steel/concrete bond might be stimulated as potentially detrimental side effects. The anodic reaction (metal dissolution) occurs where the stray current flows out from the reinforcement (anodic area) because of anodic polarization induced by current outflow. This means the process of corrosion is accelerated and cathodic reaction is depressed. In other words, corrosion of steel is initiated and accelerated in this location.

To study the effects of stray current on the corrosion behavior of steel in concrete, various works report different aspects. Nevertheless, the current state-of-the-art generally reports on anodic polarization, rather than stray current effects on the corrosion behaviour of steel in reinforced specimens [23]-[25]. Additionally, the importance of cell geometry and/or studies with respect to the orientation of the tested steel in the imposed electrical field, are not reported.

This work aimed to simulate stray-current induced corrosion for reinforced mortar and investigate the electrochemical response of the steel reinforcement with respect to the effect of reinforcement positioning. This aspect is of significance in view of the level of current that will be "picked-up" by the reinforcement. For this reason, two geometrical positions of the reinforcement were tested - steel bar placed parallel or orthogonal to the current direction. In order to account for the significant effect of environmental conditions, mainly the presence of chloride ions as a corrosion accelerator, the stray current conditions were simulated in both chloride-free and chloride-containing medium. The level of stray current was set at 3 mA/cm^2 (through the application of external DC electrical field). This paper focuses on the results from electrochemical monitoring of reinforced mortar specimens in the time frame of the test of 123 days. Several types of general or more sophisticated electrochemical tests are presented and discussed in view of the effect of stray current on the corrosion state of steel reinforcement.

II. Experimental

A. Materials and Specimens

Reinforced mortar cubes of 40mm×40mm×40mm, were cast from Ordinary Portland cement CEM I 42.5 N and normed sand. The water-to-cement (w/c) ratio was 0.5; the cement-to-sand ratio was 1:3. Construction steel (rebar) FeB500HKN (d=6mm), with exposed length of 20 mm was centrally embedded in the mortar cubes in two different geometrical arrangements - reinforcing steel placed parallel or orthogonal to the current direction, Fig. 2. The two ends of the rebars were insolated (covered by epoxy resin). Prior to casting, the steel rebars were cleaned electrochemically (cathodic treatment with 100 A/m^2 current density, using stainless steel as anode) in a solution of 75 g NaOH, 25 g Na_2SO_4, 75 g Na_2CO_3, reagent water to 1000 mL, according to ASTM G-1 [26], [27]. The schematic presentation of the specimens' geometry is depicted in Fig. 2.

The experimental set-up and electrodes' configuration for supplying stray current (with the level of 3 mA/cm^2) are also presented in Fig. 2: two Ti electrodes (MMO Ti mesh, 40mm×40 mm) cast-in within samples preparation, served as terminals for stray current application, insulated

by epoxy resin, to ease the leakage of current to surrounding electrolyte. When the stray current supply was interrupted (min 24h before electrochemical tests), the Ti electrodes served as counter electrode in a general 3-electrode set-up, where the rebar was the working electrode and an external Saturated Calomel Electrode (SCE) served as a reference electrode.

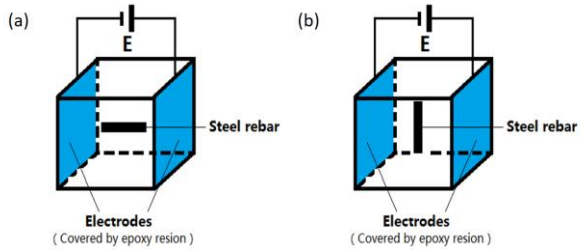

Figure 2. Schematic of test specimen and setup for stray current supply and position of electrodes: (a).steel parallel to the stray current direction; (b).steel orthogonal to the stray current direction.

After casting and prior to de-moulding and conditioning, all specimens were cured in a fog room (98% RH, 20℃) for 24 hours. The specimens were lab conditioned after demoulding. All specimens were immersed with 1/2 of their height in water or 5% NaCl solution. Table I summarizes the relevant conditions and specimens designation. It should be noted that, between 28 days to 72 days, the stray current supply was cut off, the specimens were conditioned only in water or 5% NaCl solution. After 72 days, the stray current was applied again.

TABLE I. SPECIMENS DESIGNATIONS AND RELEVANT CONDITIONS SUMMARY

Specimen designations	External environment	Steel layout (to stray current direction)
S(O)	Water (1/2)	orthogonal
S(P)	Water (1/2)	parallel
CS(O)	5% NaCl (1/2)	orthogonal
CS(P)	5% NaCl (1/2)	parallel

B. *Testing Methods*

The electrochemical measurements were performed at open circuit potential (OCP) for all specimens, using SCE as reference electrode (as above specified, the counter electrode was the initially embedded MMO Ti). The used equipment was Metrohm Autolab (Potentiostat PGSTAT302N), combined with a FRA2 module. Electro-chemical impedance spectroscopy (EIS) was employed in the frequency range of 50kHz-10mHz, by superimposing an AC voltage of 10mV (rms). Linear Polarization Resistance (LPR) was performed in the range of ±20 mV vs OCP, at a scan rate of 0.1 mV/s. Both EIS and LPR tests were performed after1, 3, 7, 14, 28, 72, 102, 116 and 123 days of conditioning. Prior to each EIS and LPR test, a 24h depolarization (potential decay) was recorded to assure stable OCP after stray current interruption. During the depolarization process and within electrochemical tests, the specimens were immersed fully in the relevant medium. At age of 72, 102, 116 and 123 days, PDP (potentio-dynamic polarization) was performed in the range of -0.15 V to +0.90 V vs OCP at a scan rate of 0.5 mV/s, in order to additionally collect information for the electrochemical state of the steel reinforcement.

III. RESULTS AND DISCUSSION

A. *OCP/ R_p Evolution with Time*

The evolution of open circuit potentials (OCP) and the evolution of polarization resistance (Rp) values, recorded via LPR measurements, can be found in Fig. 3.

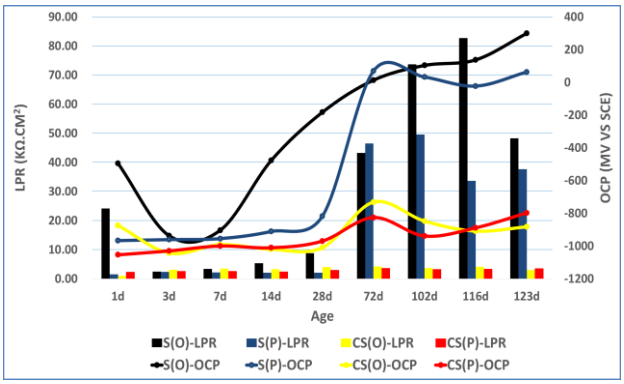

Figure 3. OCP/ R_p evolution with time (1 day to 123 days)

As expected, the OCP values of Cl^- containing specimens - CS(O) and CS(P) have remained at very negative (cathodic) levels. This, together with the recorded low R_p values, indicated the coupling effect of stray current and Cl^- ions, leading to an accelerated corrosion state of the steel rebars for the period between 1 day and 28 days.

The OCP values for specimen S(O) and S(P) shift to more noble values after 28 days reaching the range of around 0 mV vs SCE. This is in line with the trend of increasing R_p values, remaining significantly higher than those, recorded for specimens CS(O) and CS(P). However, the OCP values for the control specimens between 1 and 28 days were mostly cathodic, in the range of -500 mV to -1000 mV, which are far beyond the passivity threshold. This is due to the electrochemical cleaning prior to casting (active surface condition of the embedded steel), and in view of the "fresh" mortar matrix (only 24h fog room curing). Specifically, the lower level of maturity of the cement-based matrix in young concrete, would facilitate the stray current-induced corrosion on the steel surface, would lead to enhanced aggressive ions penetration. These effects are in addition to elevated ion and water migration due to the stray current flow. Therefore, the control specimens present an active state within the early periods of the test.

Additionally and with respect to positioning of the reinforcement in control (chloride-free) conditions, the following can be noted: after initially active surface (1 day to 3 days) in the period from 3 days onwards, specimens S(O) exhibited more anodic potentials (more noble). This was accompanied by higher R_p values (Fig. 3). In contrast, specimens S(P) presented active state, judging from both OCP and R_p values. This trend for specimens S(P) remained until 28 days. What can be concluded is that the geometrical position of the steel bar

essentially determines the electrochemical response. This is in the sense of obviously minimal, (specimens S(O)) or significant (specimens S(P)) polarization due to stray current flow. In the former case, the effect of stray current was limited to the cross section of the bar only. Consequently specimen S(O) presented higher corrosion resistance. In the latter case, the effect of stray current was significant, since the full length of the bar was exposed to the field of stray current flow. Therefore, specimens S(P) were in a more active state.

For the chloride-containing medium, specimens CS(O) and CS(P), the cell geometry and bars positioning were obviously not as significant as in control conditions. In these specimens the predominant factor, affecting steel corrosion, was the effect of chloride ions. Therefore, a clear distinction between stray current-induced corrosion and chloride-induced corrosion cannot be clearly derived within the time frame of this test.

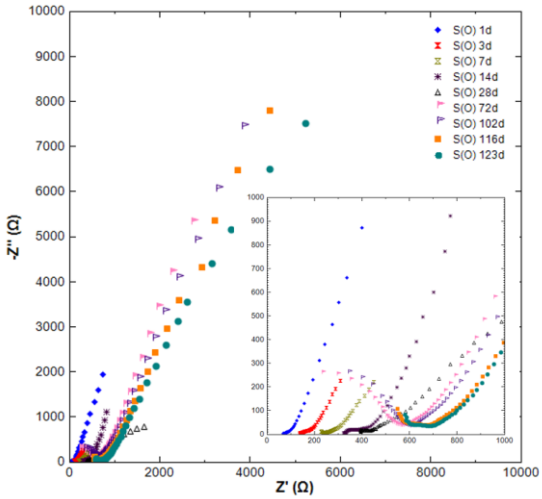

Figure. 4. EIS response for S(O) as an overlay of 1 to 123 days.

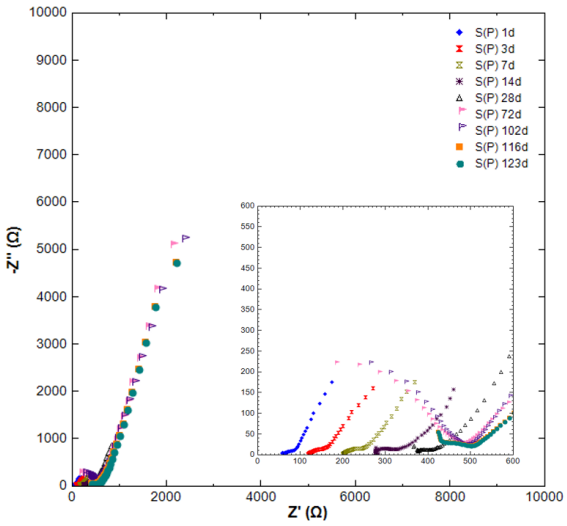

Figure. 5. EIS response for S(P) as an overlay of 1 to 123 days.

B. *Electrochemical Impedance Spectroscopy (EIS)*

The experimental impedance responses (in Nyquist format) for all groups are presented in Fig. 4 to Fig. 7 as an overlay from 1d to 123d per specimens' group (specimens geometry and active steel surface is equal, therefore normalization of the plots was not performed).

For S(O) and S(P), the shape of the experimental curves after 72 days in Fig. 4 and Fig. 5 reflect the typical response of steel in a chlorides-free cement-based environment (alkaline medium), the response depicts curves inclined to the imaginary y-axis (close to straight lines), reflecting the capacitive-like behavior, or passive state, of the steel reinforcement. This was relevant for both groups S(O) and S(P) throughout the test, denoted to stabilization of the passive layer over time. This behaviour is more significantly pronounced for the S(O) specimens, where in the LF domain (related to the steel electrochemical response) higher magnitude of impedance |Z| was recorded. The observation is in line with the OCP/R_p evolution as discussed above.

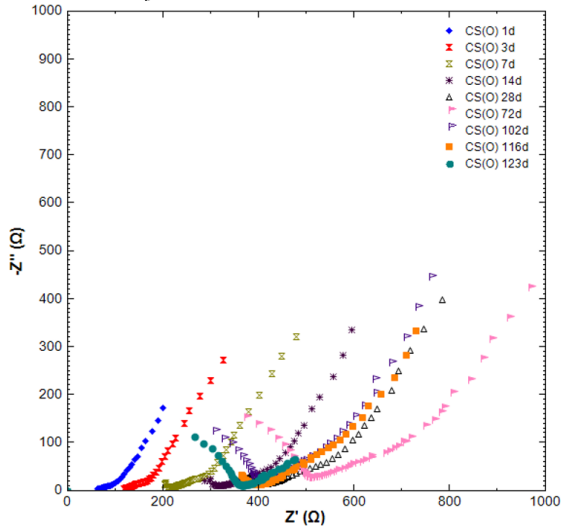

Figure. 6. EIS response for CS (O) as an overlay of 1 to 123 days.

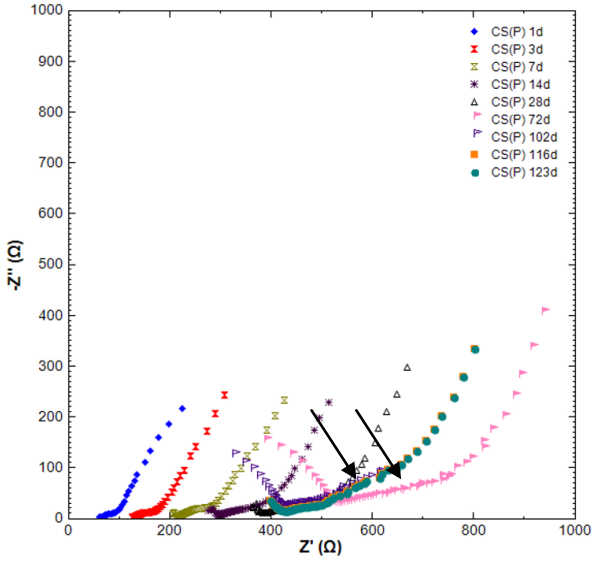

Figure. 7. EIS response for CS(P) as an overlay of 1 to 123 days.

In contrast to group S(O) and S(P), the EIS responses for groups CS(O) and CS(P) (specimens immersed in NaCl) showed clear evidence of active corrosion on the

steel surface. Starting at very early stage the response is already an inclined to the real axis semi-circle with a low magnitude of |Z| towards 123 days, clearly showing a more active state. The shape of this EIS response had been largely reported to be due to the presence of chloride ions on the steel surface and increasingly active corrosion state [28].

When it comes to the effect of steel positioning, it can be seen from the EIS response that the CS(O) and CS(P) showed very similar corrosion behavior, which is again in accordance to the above mentioned OCP/R_p evolution. Possibly, the positioning of the reinforcing steel rebar was not significant when both stray current and Cl^- ions are present. That can be attributed to the fact that at this level of stray current, the Cl^- containing environment played a more significant role on inducing steel corrosion. However, despite the fact that both groups presented similarly active response, there was an observable difference between the CS(O) and CS(P) specimens, judged form both EIS tests and later on – confirmed by PDP response. If the HF to MF response is compared in Fig. 6 and Fig. 7, what can be observed is that an additional time constant appeared, on later stages, especially pronounced for the CS(P) specimens – marked regions in Fig. 7. The initial, 1 d to 14 d response, was similar for both CS(O) and CS(P) groups. With prolonged treatment, though, the aforementioned time constant became significant for the specimens CS(P). Although a detailed analysis of the EIS results is to be performed for deriving firm conclusions on this point, the following can be stated: enhanced corrosion activity in specimens CS(P) would result in a more significant build-up of corrosion products on the steel surface. The steel surface in specimens CS(P) was affected by stray current in the full length of 2cm. In contrast, the affected by stray current steel surface in CS(O) was the cross section of the bar mainly i.e. comparatively very small. Since Cl-induced corrosion would be affecting both CS(P) and CS(O) specimens at comparable rates, the synergy of both stray current and Cl ions was expected to result in larger effects for the CS(P) specimens. While this was as initially observed, the trend was not maintained at the later stages of the experiment. Attention with this regard deserves this additional (or more pronounced) time constant in specimens CS(P), which is related to altered characteristics at the steel/cement paste interface. These alterations will in turn affect the corrosion product layer (composition and distribution) on the steel surface. In other words, concentration polarization, resistance polarization or both will contribute to the activation polarization in the case of CS(P) specimens, which would result in comparable, rather than higher corrosion activity, with respect to specimens CS(O). Limitations in the range of anodic currents for the CS(P) specimens (discussed further below with respect PDP) support this hypothesis and account for overall similar or even lower corrosion rate in specimens CS(P). This is in contrast to the expected result for a significantly more active state for CS(P), if compared to specimens CS(O).

C. Potential Dynamic Polarization (PDP)

Potentio-dynamic polarization was also performed to further clarify the observed electrochemical response. PDP polarization results are presented in Fig. 8 for the S-specimens (treated in water) and in Fig. 9 for the CS-specimens (treated in NaCl). Well observable is the difference in corrosion potentials, corrosion currents and overall PDP response between the S and CS groups, exhibiting passive state in the latter and active state in former case. The S groups (Fig. 8) presented much lower anodic currents and anodic (nobler) corrosion potentials, compared to the CS groups (Fig. 9), well in line with the previously discussed trends of OCP and Rp values evolution (Fig. 3).

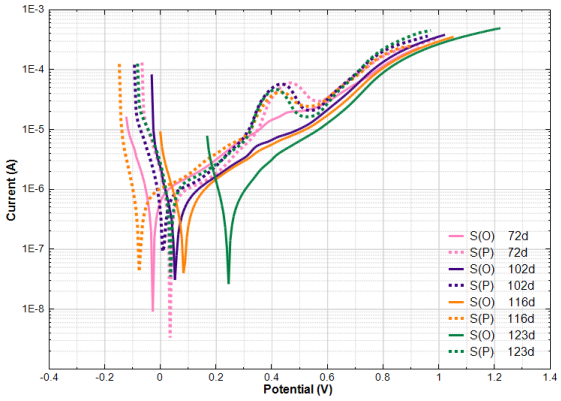

Figure. 8. PDP curves for specimens S(O) and S(P).

The steel response in both figures and conditions, respectively, can be also judged from the view point of the importance of steel orientation in the mortar cubes i.e. orthogonal or parallel to the electrical filed. Since from this perspective, and with anodic polarization, more significant differences were observed in the S groups, Fig. 8 will be discussed in more detail.

For the S groups (Fig. 8), some main features in the PDP curves are as follows: for the stages of 72 days to 123 days, the recorded corrosion potential (E_{corr}) for both S(O) and S(P) groups was mostly between -100 mV and +250 mV (SCE) i.e. in the region of passivity. More cathodic potentials were relevant for the S(P) group, however, these stabilized later-on around +30 mV at the latest stage of 123 days. For the S(O) group a relatively more cathodic potential of approx. -30 mV, was recorded at the stage of 72 days only, later on stabilized around +90 mV between 102 and 116 days. A shift to a more noble direction – approx. +250 mV, was observed at 123 days. Based on corrosion potential values, the corrosion resistance of the S(O) groups was higher than that for the S(P) group.

For the S(P) specimens, after corrosion potential and with anodic polarization, the current steadily increases up to a dynamic passive current density of approx. 0.27-0.53 $\mu A/cm^2$ (according to 3.77 cm^2 of steel surface area), which remains in a similar range between 0V and 200 mV (i.e. in the range of +30 mV to + 70 mV vs E_{corr} at each time interval). At ca. +420 mV a current maximum was observed (ca. 15.92 $\mu A/cm^2$) for the S(P) specimens,

which can be only related to a transpassive dissolution of iron oxide/ hydroxide layer, previously formed on the steel surface. Judging from thermodynamic principles, the E/pH region i.e. +420 mV/pH ~ 13 (conditions, relevant to specimens S(P)), the layer was most likely $Fe_2O_3.nH_2O$ and/or a mixture of oxide and hydroxide. The current increase above +550 mV was due to oxygen evolution.

For the S(O) group, the anodic current similarly increased after corrosion potential - a dynamic passive current, varying between 0.27 – 0.40 μA/cm^2 for 72 days and 0.29 – 0.42 μA/cm^2 for 123 days, was recorded in the region of +20 mV to +100 mV vs E_{corr} at each relevant stage. An indication for a transpassive dissolution of product layer was observed only for 72 days, with a maximum anodic current of ca. 5.31 μA/cm^2 However, with conditioning until 123 days such current maximum was not observed. Similarly to the S(P) specimens, the current increase above +550 mV was due to oxygen evolution.

What can be concluded is that for both S groups low corrosion currents were observed between 72d and 123 days and remained stable in the range of 0.08-0.16μA/cm^2, indicating passive state. This is irrespective of the orientation of the steel bar and despite the initially recorded "active" state for some specimens, together with a very different response between 1 day and 28 days, e.g. group S(P) (Fig. 3). Nevertheless, judging from the current maximum with anodic polarization for the S(P) group (Fig. 8), which was not clearly observed for the S(O) group, it can be concluded that in the case of S(P) specimens a product layer of different composition and/or distribution on the steel surface was formed, which is in the case of parallel orientation of the steel bar. This is an indication of the more significant effect of stray current in group S(P), if compared to the orthogonal direction of the steel, as in group S(O). Next to that, the anodic currents for group S(O) were lower overall, with a more significant anodic shift of corrosion potential with time. These account for the higher corrosion resistance in the S(O) group if compared to the S(P) group. The results are well in line with the EIS response in terms of magnitude of global impedance |Z|, i.e. higher |Z| was observed for group S(O), compared to group S(P) (Fig. 4 and Fig. 5). However, the response for the S(P) group, Fig. 5, is more stable over time, presenting a capacitive-like behavior, i.e. accounting for a stable passive state. In contrast, the response for the S(O) group, Fig. 4, shows an inclination to the real axis over time i.e. activity on the steel surface, although possibly related to product layer formation or transformations. In fact, the EIS results for the S(P) specimens, can be interpreted as the response of a steel surface, covered with a stable Fe^{3+}-based product layer, which is also indicated by the anodic current maximum, as observed in the PDP curves at ca. +420 mV. Obviously, a detailed analysis and quantification of EIS results is required to justify the above observations in view of the possibility to derive product layers resistance and capacitance. These, together with deriving charge transfer resistance and double layer capacitance, would already clarify variations in the product layers properties/ performance in both conditions.

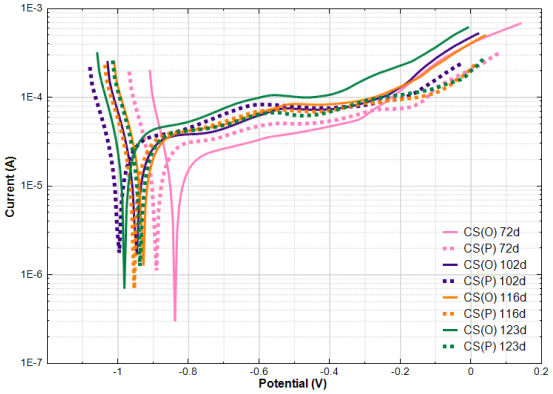

Figure. 9. PDP curves for all specimens CS(O) and CS(P)

The PDP response for the chloride-conditioned specimens CS (Fig. 9) can be summarised as follows: For the CS(O) specimens, i.e. steel in orthogonal direction, an increase in corrosion activity was observed: corrosion potentials became more cathodic, from ca. -830mV at 72 days to ca. -980mV at 123 days. This was accompanied by increase in corrosion current density from 2.65 μA/cm^2 to 7.96 μA/cm^{2}and significant increase in anodic currents – from approx. 7.96 μA/cm^2 to approx. 26.53μA/cm^2 at e.g. -600mV. The slope of the anodic curves in the potential range between +30 mV vs E_{corr} and until -200mV, in anodic direction, accounts for limitations of the anodic dissolution (although the anodic currents remain significant if compared to those for specimens S). This means that in both groups a product layer existed on the steel surface and caused limitations to the dissolution process within anodic polarisation. The effect was more pronounced in the CS (P) group, for which the increase in anodic current in time was not as significant as the CS(O) group. This behaviour, is in line with the similar corrosion current values for CS(P) between 72 and 123 days i.e. limited activity in the CS(P) group, compared to the CS(O) group.

The PDP observations are in line with the EIS response (Fig. 6 and Fig. 7), where an additional time constant was recorded for CS(P) (Fig.7). As aforementioned, this time constant is most likely denoted to a more significant accumulation of corrosion product layer and/or product layer, distributed over a larger surface in specimens CS(P). These outcomes, together with the indication for more active state of CS(P), compared to CS(O) specimens, as also recorded trough OCP and LPR (Fig. 3), denote for a larger significance of the stray current in the CS(P) group. Consequently, a more pronounced effect of the stray current was observed, when the steel is placed in parallel rather than in orthogonal position.

IV. Conclusions

This work aimed to simulate stray-current induced corrosion for reinforced mortar and investigate the electrochemical response of the steel reinforcement in

chloride-free and chloride-containing external medium. One of the main objectives of this work was to potentially justify the significance of geometrical position of the embedded reinforcement with respect to the electrical current lines of the applied electrical field. Therefore, orthogonal and parallel direction of the cast-in steel was investigated in all conditions. The level of stray current was set at 3 mA/cm^2 (through the application of external DC electrical field). The following conclusions can be drawn:

- The geometrical position of the steel bar determines the electrochemical response of the embedded steel. Orientation parallel to the electrical filed results in lower corrosion resistance i.e. a more significant effect of the stray current;
- For conditions where chloride-induced corrosion is in parallel with stray current-induced corrosion, the effect of stray current might (at first approximation) seem not significant. However, depending on the orientation of the steel reinforcement, stray current was found to induce higher corrosion activity.
- A combination of electrochemical techniques is necessary to justify the observed behavior. For example, OCP and LPR could provide valuable information and indication for the corrosion state. However, for a more in-depth investigation on related behavior, EIS and PDP are necessary.
- Quantification of the EIS response is necessary to further support the discussion on electrochemical state, as derived with anodic polarization.

ACKNOWLEDGMENT

The first author would like to express his gratitude for the financial support from Chinese Scholarship Council (CSC).

REFERENCES

[1] D. K. Kim, T. H. Ha, Y. C. Ha, J. H. Bae, H. G. Lee, D. Gopi, and J. D. Scantlebury, "Alternating current induced corrosion," *Corrosion Engineering, Science and Technology*, vol. 39, 117-123, 2004.

[2] L. Bertolini, M. Carsana, and P. Pedeferri, "Corrosion behaviour of steel in concrete in the presence of stray current," *Corrosion Science*, vol. 49, pp. 1056-1068, 2007.

[3] K. Miskiewicz, A. Wojaczek, S. Fraczek, and F. Krasucki, "Electromagnetic compatibility in underground mining: Selected problems," *Elsevier*, 2012.

[4] R. Dodds, "DC traction stray current control - A case study from a utility," *IEE Colloquium (Digest)*, 1999, pp. 49-52.

[5] D. H. Boteler and W. H. Seager, "Telluric currents: A meeting of theory and observation," *Corrosion (Houston)*, vol. 54, pp. 751-755, 1998.

[6] D. R. Lenard and J. G. Moores, "Initiation of crevice corrosion by stray current on stainless steel propeller shafts," *Corrosion (Houston)*, vol. 49, pp. 769-775, 1993.

[7] F. Brichau, J. Deconinck, and T. Driesens, "Modeling of underground cathodic protection stray currents," *Corrosion (Houston)*, vol. 52, pp. 480-488, 1996.

[8] I. A. Metwally, H. M. Al-Mandhari, A. Gastli, and A. Al-Bimani, "Stray currents of ESP well casings," *Engineering Analysis with Boundary Elements*, vol. 32, pp. 32-40, 2008.

[9] R. W. Revie, *Corrosion and Corrosion Control*, John Wiley & Sons, 2008.

[10] H. H. Uhlig, *Corrosion and Corrosion Control (Third Version) [M]*, Weng Yongji, etc. *Trans*, 1985.

[11] C. L. Wang, C. Y. Ma, and Z. Wang, "Analysis of stray current in metro DC tractionpower system," *Urban Mass Transit*, vol. 3, pp. 51-56, 2007.

[12] F. R. Wojcicki, M. E. M. Negrisoli, and C. V. Franco, "Stray current induced corrosion in lightning rod cables of 525 kV power lines towers: A case study," *Revista de Metalurgia (Madrid)*, 2003, pp. 124-128.

[13] M. Wu, "Progress of the durability of concrete structure of the subway," in *Proc. 1st International Conference on Civil Engineering, Architecture and Building Materials*, 2011, pp. 1456-1459.

[14] S. Ahmad, "Reinforcement corrosion in concrete structures, its monitoring and service life prediction - A review," *Cement and Concrete Composites*, vol. 25, pp. 459-471, 2003.

[15] Z. P. Bazant, "Physical model for steel corrosion in concrete SEA structures - application," *ASCE J. Struct Div*, vol. 105, pp. 1155-1166, 1979.

[16] T. Liu and R. W. Weyers, "Modeling the dynamic corrosion process in chloride contaminated concrete structures," *Cement and Concrete Research*, vol. 28, pp. 365-379, 1998.

[17] B. Huet, V. L'Hostis, G. Santarini, D. Feron, and H. Idrissi, "Steel corrosion in concrete: Determinist modeling of cathodic reaction as a function of water saturation degree," *Corrosion Science*, vol. 49, pp. 1918-1932, 2007.

[18] G. Santi and L. Sandrolini, "Stray current interference on high-speed rail transit systems and surrounding buried metallic structures," in *Proc. 6th Int. Congress CEOCOR*, 2003, pp. 1-12.

[19] L. Sandrolini, "Analysis of the insulation resistances of a high-speed rail transit system viaduct for the assessment of stray current interference. Part 1: Measurement," *Electric Power Systems Research*, vol. 103, pp. 241-247, 2013.

[20] L. Sandrolini, "Analysis of the insulation resistances of a high-speed rail transit system viaduct for the assessment of stray current interference. Part 2: Modelling," *Electric Power Systems Research*, vol. 103, pp. 248-254, 2013.

[21] S. L. Chen, S. C. Hsu, C. T. Tseng, K. H. Yan, H. Y. Chou, and T. M. Too, "Analysis of rail potential and stray current for Taipei Metro," *IEEE Trans. Veh. Technol*., vol. 55, pp. 67-75, 2006.

[22] A. Susanto, D. A. Koleva, O. Copuroglu, K. van Beek, and K. van Breugel, "Mechanical, electrical and microstructural properties of cement-based materials in conditions of stray current flow," *Journal of Advanced Concrete Technology*, vol. 11, pp. 119-134, 2013.

[23] C. Lingvay, A. Cojocaru, T. Vişan, and I. Lingvay, "Degradations of reinforced concrete structures due to d.c. and a.c. stray currents," *UPB Sci Bull Ser B*, vol. 73, pp. 143-152, 2011.

[24] H. W. Teng, S. M. Yang, Z. C. Shu, Y. Huang, and D. Huo, "Simulation experiment of loading influence to reinforcement corrosion affected by stray current and salt solution," *Wuhan Ligong Daxue Xuebao*, vol. 32, pp. 147-151, 2010.

[25] S. J. Duranceau, W. J. Johnson, and R. J. Pfeiffer-Wilder, "A study examining the effect of stray current on the integrity of continuous and discontinuous reinforcing bars," *Experimental Techniques*, vol. 35, pp. 53-58, 2011.

[26] "Standard practice for preparing, cleaning, and evaluating corrosion test specimens," Annual Book of ASTM Standards, 2003, pp. 17-25.

[27] C. Alonso, M. Castellote, and C. Andrade, "Chloride threshold dependence of pitting potential of reinforcements," *Electrochimica Acta*, vol. 47, pp. 3469-3481, 2002.

[28] D. A. Koleva, K. van Breugel, J. H. W. de Wit, E. van Westing, N. Boshkov, and A. L. A. Fraaij, "Electrochemical behavior, microstructural analysis, and morphological observations in reinforced mortar subjected to chloride ingress," *Journal of the Electrochemical Society*, vol. 154, p. E45, 2007.

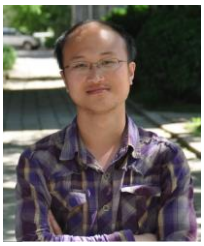

Zhipei Chen PhD candidate in material and environment section, structure engineering department- Civil Engineering and Geoscience faculty- Delft University of Technology (TU Delft), Netherlands.
Bachelor in Civil Engineering (2010), School of Human Settlements and Civil Engineering, Xi'an Jiaotong University, China.
Master in Structural Engineering, School of Civil Engineering, Dalian University of Technology, CHINA.